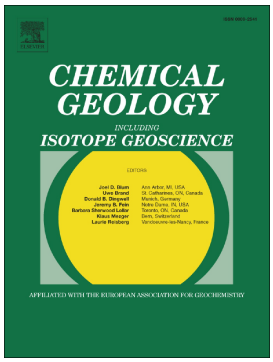

Clumped and stable isotopes of land snail shells on the Chinese Loess Plateau and their climatic implications

Jibao Dong, John Eiler, Zhisheng An, Naiqin Wu, Weiguo Liu, Xiangzhong Li, Nami Kitchen, Fengyan Lu

PII: S0009-2541(19)30543-1

DOI: https://doi.org/10.1016/j.chemgeo.2019.119414

Reference: CHEMGE 119414

To appear in: *Chemical Geology*

Received date: 4 May 2019

Revised date: 11 November 2019

Accepted date: 18 November 2019

Please cite this article as: J. Dong, J. Eiler, Z. An, et al., Clumped and stable isotopes of land snail shells on the Chinese Loess Plateau and their climatic implications, *Chemical Geology* (2019), https://doi.org/10.1016/j.chemgeo.2019.119414

Clumped and stable isotopes of land snail shells on the Chinese Loess Plateau and their climatic implications

Jibao Dong[1,2,*], John Eiler[3], Zhisheng An[1, 2], Naiqin Wu[4], Weiguo Liu[1], Xiangzhong Li[1], Nami Kitchen[3], Fengyan Lu[1]

[1] *State Key Laboratory of Loess and Quaternary Geology, Institute of Earth Environment, Chinese Academy of Sciences, 710061 Xian, China.*

[2] *CAS Center for Excellence in Quaternary Science and Global Change, Chinese Academy of Sciences, 710061 Xian, China.*

[3] *California Institute of Technology, Pasadena, CA 91125, USA*

[4] *Key Laboratory of Cenozoic Geology and Environment, Institute of Geology and Geophysics, Chinese Academy of Sciences, Beijing 100029, China*

** Corresponding to Jibao Dong djb@ieecas.cn;*

Abstract

We report stable ($\delta^{13}C_{shell}$, $\delta^{18}O_{shell}$) and clumped isotope (Δ_{47}) compositions of modern and last glacial fossil snail shell carbonates from the Luochuan and Weinan sections on the central and southern Chinese Loess Plateau (CLP). Our study reveals that the average Δ_{47} temperature (T_{47}) of modern snails is consistent with monitored temperatures during the snail growing season at the studied locations and is ~10 ℃ higher than that of fossil snails from glacial time. Moreover, the average $\delta^{13}C_{shell}$ of modern snails is more depleted than that of fossils. We argue that the $\delta^{13}C_{shell}$ cannot record changes in plant communities (i.e., the C3/C4 ratio) on the CLP and may mainly indicate arid conditions with depleted values reflecting reduced aridity. Additionally, the reconstructed snail body water $\delta^{18}O$ ($\delta^{18}O_{water}$) of modern snails is more enriched than $\delta^{18}O$ in modern growing season precipitation and $\delta^{18}O_{water}$ of fossils. This contrast may be related to the high degree of evaporative enrichment of environmental water ^{18}O in the body/ingested by modern snails under warm conditions. Therefore, we suggest that using $\delta^{18}O_{shell}$ to directly reconstruct the oxygen isotopes of precipitation is difficult and that higher $\delta^{18}O_{shell}$ and $\delta^{18}O_{water}$ values probably indicate higher environmental temperature/stronger evaporative enrichment on glacial-interglacial timescales on the CLP.

Key words: Clumped isotopes; Stable isotopes; Land snail; Temperature; Chinese Loess Plateau (CLP)

1. Introduction

Widespread land snails are regarded as a valuable archive for studying environmental and climatic conditions because of their high sensitivity to temperature and humidity (Liu, 1985; Goodfriend, 1992; Wu et al., 2018). Moreover, their fossil remains are abundant in Quaternary deposits, such as the loess-paleosol sequences on the Chinese Loess Plateau (CLP), and they are considered typical 'index animals' in paleoenvironmental studies (Liu, 1985; Wu et al., 2018). Thus, snail faunal assemblages (Goodfriend 1992; Rousseau and Wu 1997; Wu et al., 2002, 2018) and isotopic compositions of snail shell carbonates (Goodfriend 1992; Bonadonna and Leone 1995; Abell and Plug 2000; Goodfriend and Ellis 2000; Balakrishnan et al., 2005a; Colonese et al., 2010, 2013; Kehrwald et al. 2010; Yanes et al., 2011, 2013a, b, 2014, 2017; Huang et al., 2012; Prendergast et al., 2016) have been widely used to decipher past climatic and environmental changes.

Many studies have suggested that the carbon isotope composition of land snail shell carbonate ($\delta^{13}C_{shell}$) is derived from three potential sources: diet, atmospheric CO_2, and ingested carbonates (Goodfriend and Hood 1983; Pigati et al., 2004; Quarta et al., 2007; Romaniello et al., 2008; Xu et al., 2011; Zhang et al., 2014). Laboratory studies indicated that the $\delta^{13}C_{shell}$ reflects mostly the respired CO_2 derived from ingested plants (Stott, 2002; Metref et al., 2003; Zhang et al., 2014). Thus, most published field investigations of modern/fossil land snails assume that they primarily consumed C3 and C4 plants in relation to their abundances in the surrounding environment, and $\delta^{13}C_{shell}$ has therefore traditionally been used to deduce variations in

C3/C4 plants in the landscape (Goodfriend and Ellis 2000, 2002; Balakrishnan et al. 2005a, b; Liu et al., 2007; Yanes et al. 2008, 2009, 2011, 2013b, 2014; Colonese et al. 2014; Prendergast et al., 2017). $\delta^{13}C_{shell}$ can also be applied to infer changes in aridity in C3-dominated landscapes (Colonese et al., 2013; Prendergast et al., 2017). However, snails show a preferential use of C3 food when fed a mixed diet (Metref et al., 2003; Zhang et al., 2014). Moreover, radiocarbon dating work has indicated that carbon from ingested carbonates and atmospheric CO_2 may also contribute to snail shells (Goodfriend and Stipp 1983; Pigati et al., 2004; Quarta et al., 2007; Romaniello et al., 2008; Xu et al., 2011). These additions complicate the explanation of $\delta^{13}C_{shell}$ from the perspective of climatic and environmental changes because the relative contributions from the three potential sources remain unclear.

Pioneering attempts showed that the oxygen isotope compositions of land snail shells ($\delta^{18}O_{shell}$) were inversely related to local relative humidity (Yapp et al., 1979). Goodfriend et al. (1989) and Baldini et al. (2007) found that the isotopic compositions of snail body water ($\delta^{18}O_{body\ water}$) and $\delta^{18}O_{shell}$ were influenced by atmospheric water vapor. Other studies illustrated relationships between the oxygen isotope composition of meteoric water and those of land snail shells (Lécolle 1985; Goodfriend et al., 1989; Zanchetta et al., 2005; Yanes et al., 2009, 2017; Colonese et al., 2014; Prendergast et al., 2015). Zhang et al. (2018) suggested that food water should also be considered a water source, apart from rainwater. Thus, the flux balance model proposed that the $\delta^{18}O$ value of snail shell carbonate represented the combined effects of the relative humidity, $\delta^{18}O$ of ingested water (e.g., precipitation), and temperature at which the

shell precipitated (Balakrishnan and Yapp, 2004). Overall, the explanation of the oxygen isotopes of land snail shells is more complex than that of the carbon isotopes due to the variable temperature, relative humidity and $\delta^{18}O$ of water in the terrestrial environment.

The newly developed carbonate clumped isotope (expressed as Δ_{47}) thermometry technique was proposed to quantitatively reconstruct the temperature of carbonate mineral growth under isotopic equilibrium conditions (Ghosh et al., 2006, Eiler 2007). This technique is based on the abundance of $^{13}C–^{18}O$ bonds in the carbonate lattice relative to those expected for a random distribution of isotopes among all isotopologues and is independent of the $\delta^{18}O$ of the waters from which carbonates grew (Ghosh et al., 2006, Eiler 2007). Recently, published data on different carbonate minerals of biogenic/inorganic origin demonstrated that Δ_{47} generally follows a universal Δ_{47}-temperature calibration (Bonifacie et al., 2017; Kelson et al., 2017). Therefore, we apply this thermometry to simultaneously obtain the shell formation temperature and the $\delta^{18}O_{body\ water}$ of land snails in combination with $\delta^{18}O_{shell}$, both of which are indispensable for understanding the stable isotope composition of snail shells.

However, current studies showed discrepant results when converting snail shell clumped isotopes to land snail shell calcification temperature (T_{47}) or the environmental temperature. For example, Zaarur et al. (2011) indicated that T_{47} values of snail shells are typically higher than either the mean annual or the snail activity season ambient temperatures. In contrast, Eagle et al. (2013) and Wang et al. (2016)

revealed that T_{47} values for land snails are strongly correlated with environmental temperatures, although they are still higher than the local warm month mean temperatures for *Cathaica sp.* and *Bradybaena sp.* (Wang et al., 2016). Recent work by Zhai et al. (2019) and Guo et al. (2019) also reported higher than expected T_{47} versus either environmental temperatures or estimated snail activity temperatures. Furthermore, snail culturing experiments suggested that Δ_{47} of *Acusta despecta* land snails can be used to reconstruct the mean seasonal temperature of snail activity (Zhang et al., 2018). In this context, the Δ_{47} values of modern and fossil snails deserve further investigation.

Therefore, we comprehensively studied the clumped and stable isotopes (Δ_{47}, $\delta^{13}C_{shell}$, $\delta^{18}O_{shell}$, and $\delta^{18}O_{body\ water}$) of modern and last glacial fossil land snail shells from the Luochuan and Weinan sections on the central and southern CLP. The aims of this study are 1) to quantitatively reconstruct the temperature changes from the last glacial to modern time using the clumped isotope technique and 2) to further understand the climatic implications of $\delta^{13}C_{shell}$ and $\delta^{18}O_{shell}$ as well as $\delta^{18}O_{body\ water}$ on the CLP on glacial-interglacial timescales.

2. Materials and methods

The Luochuan (35.7° N, 109.4° E) and Weinan (34.5° N, 109.6° E) sections are located in the center and on the southern edge of the Chinese Loess Plateau (CLP), respectively, and the linear distance between the two sections is ~150 km (Figure 1). Approximately 15 kg of sediment was excavated at 10 cm intervals from both profiles since the last interglacial (S1 paleosol). The sediments of each sample were washed

and sieved in the field on a 0.5 mm mesh sieve, and the fossil snail shells were picked out and further ultrasonically washed in distilled water in the laboratory. The species were identified under a binocular microscope (see details of species classifications in Wu et al. (2018)). We also sampled bulk sediments at 5 cm intervals for magnetic susceptibility (MS) analysis. The MS was determined with a portable Bartington magnetometer at the Institute of Earth Environment, Chinese Academy of Sciences, and was used for stratigraphic comparison between the two sections. In addition, modern snail shells were collected near the sections.

For the clumped isotope measurements, the fresh modern snail shells were treated with 3% H_2O_2 for ~1 hour at room temperature to remove organic components and then rinsed in distilled water. The fossil snail shells were ultrasonically cleaned in distilled water, and only the glassy shells were selected for clumped isotope analysis because glassy shells suggest that they have not been reworked and preserve original climatic information. Several whole shells of minute species (<2 mm, e.g., *P. aeoli* and *V. tenera*) were used for clumped isotope analysis, while only parts of the large shells (>10 mm, e.g., *C. pulveraticula*, *C. pulveratrix*, *M. yantaiensis*, and *M. huaiensis*) were well preserved, usually the shell mouth part, which is formed when snail approaches adulthood. All shells were air-dried at room temperature and crushed into homogeneous powders using an agate mortar.

The clumped isotope measurements were performed in 2012 for fossil snails and in 2012 and 2017 for modern snails at Caltech. There was only 1 measurement for each sample. The purified CO_2 samples were analyzed using a Thermo Scientific

MAT253 mass spectrometer at Caltech, which was configured to simultaneously collect ion beams corresponding to m/z = 44, 45 and 46 (read through 10^8 Ohm to 10^{11} Ohm resistors), as well as 47, 48 and 49 (read through 10^{12} Ohm resistors), and the voltage for m/z 44 was set to 16 V (Eiler (2004). There were 7 cycles (26 s integration time for each cycle) and 8 acquisitions for analyzing each sample. This approach corresponded to an ~1500 s integration time for each sample. Approximately 8 mg of sample was reacted in a common phosphoric acid bath for 20 min at 90 ℃. The extracted CO_2 was passed through an ethanol/dry ice U-trap (~80 ℃) before collection in a liquid nitrogen U-trap. Thereafter, the sample CO_2 was passed through a Porapak Q 120/80 mesh gas chromatography column held at -20 ℃ for a period of 15 min using helium (~25 mL/min) as the carrier gas. CO_2-equilibrium gases were prepared by equilibrating CO_2 gases with water of different isotopic compositions for more than three days. The heated gases were prepared by heating CO_2-equilibrium gases at 1000 ℃ for more than 3 hours and were then quickly quenched at room temperature. All the heated and CO_2-equilibrium gases were purified as the powder samples were and then analyzed using a MAT253 mass spectrometer. The isotopic composition of the reference gas was $\delta^{13}C$=3.62‰ (PDB) and $\delta^{18}O$=24.97‰ (SMOW). We calculated the Δ_{47} values by applying the ^{17}O correction parameters from Brand et al. (2010), as suggested by Daëron et al. (2016) and Schauer et al. (2016), and reported them on the carbon dioxide equilibrated scale (CDES) (Dennis et al., 2011). For the samples analyzed in 2012, the heated gases and standards of CIT Carrara (Δ_{47}=0.316 without acid correction) and TV01 (Δ_{47}=0.629

without acid correction) were used to transfer raw Δ_{47} data to the CDES frame. For the samples analyzed in 2017, CO_2-equilibrium gases and heated gases were used to transfer raw Δ_{47} data to the CDES frame and then corrected by the standards CIT Carrara and TV04 (Δ_{47}= 0.563 without acid correction). All data were processed on the website http://rambaldi.pythonanywhere.com/.

3. Results

Table 1 presents the stable isotope values and clumped isotope without acid fractionation correction ($\Delta_{47CDES90}$) results for fossil and modern shells analyzed in 2012 and 2017 at Caltech, as well as the calculated snail body water isotope and clumped isotope temperature (T_{47}). The $\delta^{18}O_{water}$ was calculated using the aragonite–water fractionation proposed by Kim et al. (2007), and the Δ_{47}–T calibration line and the acid fractionation factor of 0.088 in Peterson et al. (2019), who reprocessed data from 11 different laboratories using the Brand et al. (2010) parameters, were used to convert $\Delta_{47CDES90}$ to T_{47}. We acknowledge that a recent study by Zhang et al. (2019) reported a solid calibration in Brand et al. (2010) parameters, which could also be applied to our data, and this study does not affect our conclusion.

We compare the stable and clumped isotope results between the two sections and among different species in the same section, as well as different shell sizes, e.g., large (>10 mm) versus minute (<2 mm). No obvious differences are observed (Table 1, Figure 2 and supplementary Figures S1, S2). Thus, we focus our discussion on the combined results of all fossils from the two sections and treat them as an integrated glacial record, and the pooled modern snail results are treated as an interglacial record.

We also attempt to establish the time series variations in T_{47} by averaging at least two measurements of fossil snails at the same depth from the Weinan and Luochuan sections. They display similar fluctuations (~4 ℃) from MIS 4 to MIS 3, although this amplitude is on the same order of magnitude as the analytical precision (Figure 3).

For the modern snails, the $\Delta_{47CDES90}$ averages 0.593±0.017‰ (corresponding T_{47} is 28±6 °C) (Figure 4). The $\delta^{13}C_{shell}$ ranges from -8.2‰ to -14.6‰ with a mean value of -10.3‰ (Figure 5). The mean $\delta^{18}O_{shell}$ averages -3.5‰ (from -0.5‰ to -9.4‰) (Figure 6). The mean $\delta^{18}O_{water}$ is -1.4‰ (Figure 7) and is more enriched in ^{18}O than the precipitation during the snail growing season on the CLP (mean value of -6.9‰ at Xi'an from April to October, varying from ~-4.5‰ to ~-9.4‰, from http://isohis.iaea.org).

The $\Delta_{47CDES90}$ of all fossil snails from Weinan and Luochuan varies from 0.594‰ to 0.651‰ with a mean value of 0.629±0.017‰, and the corresponding T_{47} ranges from 9 ℃ to 27 ℃ with a mean T_{47} of 16±6 ℃ (Figure 4). The $\delta^{13}C_{shell}$ averages -7.6‰, ranging from -6.1‰ to -9.1‰ (Figure 5), and the mean $\delta^{18}O_{shell}$ is -6.3‰, varying between 0.2‰ and -13.1‰ (Figure 6). Correspondingly, the mean $\delta^{18}O_{water}$ is -6.5‰ (Figure 7).

4. Discussion

4.1 Clumped isotopes of snails

Previous studies reported that the T_{47} of modern snails is higher than the mean annual temperature and even higher than the growing season temperature (GST), and this phenomenon was attributed to snail eco-physiological adaptations (Zaarur et al.,

2011; Wang et al., 2016, 2019; Guo et al., 2019). In contrast, our results show that both the range and mean values of T_{47} for our modern snails are very close to the temperature from April to October when the monthly average T is greater than 10 ℃ and precipitation is abundant in the study area and that all shell T_{47} values are >10 ℃ with only three samples >30 ℃ (Table 1, Figure 2). These results are consistent with the observations that snails become inactive at temperatures less than 10 ℃ (Thompson and Cheny, 1996) and that high temperatures (>30 ℃) cause inactive or estivating snails (Xu et al., 2002). Furthermore, a recent culturing experiment demonstrated that the Δ_{47} values of land snails lie within the uncertainties of the published Δ_{47}–T calibration line of Kelson et al. (2017), indicating that the shells' Δ_{47} values record their formation temperatures without noticeable offset (Zhang et al., 2018). Therefore, we suggest that our modern snail shell T_{47} reflects the environmental temperature from April to October or the GST in the study areas when the climate is characterized by relatively warm temperatures (monthly average T >10 ℃) and precipitation (Figure 2, Figure 8).

To date, only Eagle et al. (2013) have analyzed clumped isotopes on fossil *Cathaica sp.* shell aragonites, and they reconstructed a temperature difference of ~7 ℃ between the last glacial maximum (LGM) and the present on the CLP. We analyzed more fossil species (Table 1) from two sections on the central and southern CLP, and the data cover longer time periods from MIS 4 to early MIS 2 (Figure 3). Moreover, the T_{47} variations are quite similar in the two sections, which are ~150 km apart (Figure 3). These factors strengthen the reliability of our results. Our fossils' T_{47} averages 16 ℃,

ranging from 9 ℃ to 27 ℃, which is ~10 ℃ lower than those of their modern counterparts (~28 ℃, Table 1, Figures 2 and 3). Our data further might indicate an ~4 ℃ increase from stadial (MIS 4) to interstadial time (MIS 3), although this amplitude is on the same order of magnitude as our measurement error (Figure 3). This observation implies that the T differences between the LGM and the present may have been even larger (>10 ℃). This argument is further supported by a pollen study indicating a temperature offset up to 13 ℃ from the LGM to the present (An et al., 1990). In addition, a fossil assemblage study suggests that seasonality was strengthened during the LGM (Wu et al., 2002). This situation would further bias the T_{47} of LGM fossils toward the warm season and decrease the reconstructed temperature offset. Overall, we argue that the modern GST is more than 10 ℃ higher than that during the LGM on the CLP.

4. 2 Carbon isotopes

Our mean fossil snail $\delta^{13}C_{shell}$ is 2.7‰ more positive than that of modern snails (Figure 5). This offset may reflect carbon source changes (diet, atmospheric CO_2 and carbonate rocks) on glacial-interglacial timescales. A similar phenomenon was reported previously and explained in terms of water-stressed vegetation or a large proportion of C4 plants (Yanes et al., 2011, 2013b, Colonese et al., 2013). Accordingly, this offset indicates that the fossils collected from the glacial loess deposits may have consumed more C4 or water-stressed plants, which have more positive carbon isotopes (Kohn 2010). However, stable carbon isotope studies on soil organic matter and soil carbonates suggest that the proportion of C4 plants increased

during warm-humid interglacial periods on the CLP (An et al., 2005, Liu et al., 2005). This observation implies that modern snails should have more opportunities for consuming C4 plants than the fossil snails had in the glacial period. Thus, our results cannot be explained by variations in C4 plant fractions on glacial-interglacial timescales.

Another possibility is that fossil snails may have ingested more water-stressed C3 plants during glacial periods than their modern counterparts (Colonese et al., 2013) because the $\delta^{13}C$ values of water-stressed C3 plants tend to be relatively positive (Kohn 2010). Culturing experiments suggest the preferential use of C3 food by snails (Metref et al. 2003; Zhang et al., 2014). Considering that the $\delta^{13}C$ of modern C3 plants exhibits a negative correlation with annual precipitation with a slope of -1.1‰/100 mm on the CLP (Liu et al., 2005), ~250 mm precipitation changes would induce 2.7‰ variations in $\delta^{13}C_{shell}$ in this study. This scenario is also supported by reconstructed paleoprecipitation variations on glacial-interglacial timescales on the CLP (Zhou et al., 2014). Therefore, the $\delta^{13}C_{shell}$ values may serve as a proxy for paleoprecipitation or aridity changes (Goodfriend and Magaritz, 1987; Goodfriend, 1992; Goodfriend and Ellis, 2000, 2002). This argument is also consistent with the positive $\delta^{13}C_{shell}$ values for northerly species and negative values for southerly species in the East Asian monsoon region of China (Bao et al., 2018) if carbonate ingestion is not the prime factor for this difference.

According to a previous study (An et al., 2005; Liu et al., 2005), $\delta^{13}C$ of carbonates in the surface soils should be relatively more enriched than that in the

glacial loess on the CLP. If $\delta^{13}C_{shell}$ were strongly influenced by soil carbonates, we should observe positive $\delta^{13}C_{shell}$ for modern snails and negative $\delta^{13}C_{shell}$ for fossils, not the opposite. This result implies that the incorporation of carbonates could not significantly affect the offset in mean $\delta^{13}C_{shell}$ between fossil and modern snails, although it produces anomalous radiocarbon dating results due to the "limestone effect" (Goodfriend and Stipp 1983). Thus, the influences of soil carbonate cannot reconcile the phenomena observed in this study.

On glacial-interglacial timescales, the variations in $\delta^{13}C$ of atmospheric CO_2 ($\delta^{13}C_{atm}$) may also cause changes in $\delta^{13}C_{shell}$. The $\delta^{13}C_{atm}$ derived from ice cores demonstrate that the $\delta^{13}C_{atm}$ was -6.5‰ to -7‰ during glacial time (Schmitt et al., 2012), which is more positive than the modern atmospheric CO_2 (-8‰) due to the Suess effect (Eide et al., 2017). Snails may directly incorporate atmospheric CO_2 into their shell carbonate via respiration (Goodfriend and Hood 1983; Zhang et al., 2014). Moreover, the $\delta^{13}C_{atm}$ signal may also be recorded in plant $\delta^{13}C$, which may finally be indirectly transferred into snail shells. However, this shift in $\delta^{13}C_{atm}$ cannot fully explain the observed $\delta^{13}C_{shell}$ changes. In addition, lower temperatures may cause larger carbon isotope fractionation during photosynthesis (O'Leary, 1981) and thus lower $\delta^{13}C$ values in plants (Wang et al., 2013). This process may counteract the effect of higher $\delta^{13}C_{atm}$ values. Hence, the $\delta^{13}C_{atm}$ variations may partly account for the changes in $\delta^{13}C_{shell}$ in our record.

Furthermore, large temperature changes on glacial-interglacial timescales should also be considered in understanding the $\delta^{13}C_{shell}$ variations, although the

temperature-dependent carbon isotope fractionation is not large (-0.114 ‰/℃; Romanek 1992; Zhang et al., 1995). Our T_{47} shows that the mean snail growing season temperature was ~10 ℃ lower during glacial time (Figure 5). Such a large temperature decrease causes ~1.1‰ more positive $\delta^{13}C_{shell}$ for fossils due to temperature-dependent fractionation during the precipitation of aragonite shells (Romanek 1992; Zhang et al., 1995). This conclusion is also supported by the negative correlation between $\delta^{13}C_{shell}$ and T_{47} with a slope of -0.15 ‰/℃ (Figure 9), which is close to the carbon isotope fractionation model prediction (Stott 2002). This result was also reported by Zhang et al. (2014) in their cultivated land snails, with a slope of ~-0.17‰/℃. However, this temperature effect can explain only 36% of the variance of $\delta^{13}C_{shell}$. Consequently, temperature may not be the main factor explaining $\delta^{13}C_{shell}$ changes. Moreover, there is a positive relationship between the $\delta^{13}C$ values of C3 plants and the mean annual temperature (-0.104 ‰/℃; Wang et al., 2013). This relationship implies that low temperatures lead to negative $\delta^{13}C$ in C3 plants and ultimately to negative $\delta^{13}C_{shell}$. The two aspects of temperature effects may counteract each other in some way and may attenuate the influence of temperature on glacial-interglacial timescales.

Overall, we suggest that $\delta^{13}C_{shell}$ probably cannot record changes in plant communities (i.e., the ratio of C3/C4 plants) on glacial-interglacial timescales on the CLP and may respond mainly to aridity conditions, with negative values reflecting reduced aridity. Changes in $\delta^{13}C_{atm}$ and temperature may also partly impact $\delta^{13}C_{shell}$.

4.3 Oxygen isotopes

If the offset between $\delta^{18}O_{shell}$ and local $\delta^{18}O_{precipitation}$ is spatially and temporally constant, $\delta^{18}O_{shell}$ may be used to reconstruct $\delta^{18}O_{precipitation}$ for the past. However, the considerable variation (2-8‰) in the reported offsets (Prendergast et al., 2015; Colonese et al., 2014; Yanes et al., 2009; Zanchetta et al., 2005; Goodfriend and Ellis, 2002; Goodfriend et al., 1989; Goodfriend and Magaritz, 1987; Lécolle 1985) restricts its wide application. For our study, the large range of our $\delta^{18}O_{shell}$ (~9‰) in both modern and glacial fossil snails make reconstructing $\delta^{18}O_{precipitation}$ even more difficult in arid-semiarid regions influenced by the Asian summer monsoon (Figure 6). Moreover, our reconstructed mean $\delta^{18}O_{body\ water}$ of modern snails (-1.4‰) is also more enriched than the growing season $\delta^{18}O_{precipitation}$ on the CLP (Figure 8), and it is even more enriched than the reported $\delta^{18}O$ of dew in northwest China (Wen et al., 2012). Although the large variability may be related to environmental variations at the habitat level and the mean value of numerous shells may express the mean climatic conditions, such large changes in $\delta^{18}O_{shell}$ and $\delta^{18}O_{body\ water}$ cannot be fully explained by the fluctuation in precipitation $\delta^{18}O$ during the snail growing season on the CLP (Figure 8).

Interestingly, the most negative $\delta^{18}O_{body\ water}$ of modern snails seems to represent the closest estimate for $\delta^{18}O_{precipitation}$ on the CLP, similar to that reported by Yanes et al. (2008). This result further reveals that snail body water is more enriched in $\delta^{18}O$ than the original intake water due to evaporative enrichment (Zaarur et al., 2011) because land snails are susceptible to dehydration by losing water via evaporation. This phenomenon is also consistent with the idea that steady-state evaporation

enriches body water in $\delta^{18}O$ (Yapp 1979, Balakrishnan and Yapp, 2004). Therefore, when reconstructing $\delta^{18}O_{precipitation}$ using $\delta^{18}O_{shell}$, it is necessary to understand the degree of evaporative enrichment, which is related to the relative humidity and environmental temperature (Balakrishnan and Yapp, 2004).

According to the model of Balakrishnan and Yapp (2004), the positive shift in $\delta^{18}O_{body\ water}$ for modern snails may be related to changes in relative humidity, temperature and $\delta^{18}O$ of ingested water (e.g., precipitation) on glacial-interglacial timescales. The $\delta^{18}O_{precipitation}$ may be more depleted during glacial time due to the "temperature effect" (Rozanski et al., 1992; Figure 4), and the relative humidity may also be higher under lower temperature conditions. Correspondingly, modern $\delta^{18}O_{precipitation}$ may be more positive, and relative humidity might be lower. This scenario seems reasonable to account for our data. However, the precipitation $\delta^{18}O$ is strongly controlled by the air mass trajectory, which mainly comes from the Asian summer monsoon (ASM) in the study area, and its $\delta^{18}O$ is suggested to be more depleted during strong monsoon periods in interglacial time (Cheng et al., 2016, Zhang et al., 2017). Thus, the $\delta^{18}O$ of the water source should be similar or more depleted for modern snails than for glacial fossils. Therefore, we suggest that the positive shifts in $\delta^{18}O_{shell}$ and $\delta^{18}O_{water}$ are mainly caused by high temperature/strong evaporative enrichment during interglacial periods, which may overwrite the original isotopic signal of the source water.

In summary, we suggest that $\delta^{18}O_{shell}$ cannot be directly related to $\delta^{18}O_{precipitation}$ on glacial-interglacial timescales on the CLP. The enriched $\delta^{18}O_{shell}$ and $\delta^{18}O_{body\ water}$

probably indicate higher environmental temperature/strong evaporative enrichment on the CLP.

5. Conclusions

We studied the clumped and stable isotopes ($\delta^{13}C_{shell}$, $\delta^{18}O_{shell}$, and $\delta^{18}O_{water}$) of modern land snail shells and fossil snail shells from the last glacial period at the Luochuan and Weinan sections on the CLP. Contrary to previous studies, our study shows that the clumped isotope temperature of snail shells is consistent with the snail growing season temperature at the studied locations and that it is ~10 ℃ lower for last glacial fossil snails than for their modern counterparts. Moreover, we argue that the $\delta^{13}C_{shell}$ cannot reflect the C3/C4 changes on the CLP and may be related to the aridity conditions with negative values reflecting reduced aridity. Furthermore, the reconstructed $\delta^{18}O$ of modern snail body water is more positive than the growing season precipitation isotopes and those of the fossils. We suggest that it is difficult to use $\delta^{18}O_{shell}$ to directly reconstruct the oxygen isotopes of precipitation due to varying degrees of evaporative enrichment of water ^{18}O under variable microenvironments and that higher $\delta^{18}O_{shell}$ and $\delta^{18}O_{water}$ values probably indicate higher environmental temperature/lower relative humidity on glacial-interglacial timescales on the CLP.

Acknowledgments

We sincerely thank professor Peter Hale Molnar for comments on and revision of the manuscript, and we thank Dr. Linpei Huang for help in the identification of fossil snail species and Dr. Ryb Uri and Dr. Max Lloyd for help with data processing and discussion. This work was jointly supported by grants from the Training Program of the State Key Laboratory of Loess and Quaternary Geology, Chinese Academy of Sciences (QYZDY-SSW-DQC001 and ZDBS-SSW-DQC001), the MOST program (2016YFE0109500), the National Natural Science Foundation of China (41430103 and 41302152) and grants EAR-0909199 and EAR 1211378.

References

Abell, P.I., Plug, I. (2000) The Pleistocene/Holocene transition in South Africa: evidence for the Younger Dryas event. *Global & Planetary Change* **26**, 173-179.

An, Z.S., Huang, Y., Liu, W., Guo, Z., Steven, C., Li, L., Warren, P., Ning, Y., Cai, Y., Zhou, W., Lin, B., Zhang, Q., Cao, Y., Qiang, X., Chang, H., Wu, Z. (2005) Multiple expansions of C_4 plant biomass in East Asia since 7 Ma coupled with strengthened monsoon circulation. *Geology* **33**, 705-708.

An, Z.S., Wu, X.H., Lu, Y.C., Zhang, D.E., Sun, X.J., Dong, G.R. (1990) A preliminary study on the paleoenvironment change of China during the last 20,000 years in: Liu, T.S. (Ed.), Loess, Quaternary Geology and Global Change Part II, pp. 1-26.

Balakrishnan, M., Yapp, C.J. (2004) Flux balance models for the oxygen and carbon isotope compositions of land snail shells. *Geochimica Et Cosmochimica Acta* **68**, 2007-2024.

Balakrishnan, M., Yapp, J.C., Meltzer, J.D., Theler, L.J. (2005a) Paleoenvironment of the Folsom archaeological site, New Mexico, USA, approximately 10,500 ^{14}C yr B.P. as inferred from the stable isotope composition of fossil land snail shells. *Quaternary Research* **63**, 31-44.

Balakrishnan, M., Yapp, J.C., Theler, L.J., Carter, J.B., Don, G.W. (2005b) Environmental significance of $^{13}C/^{12}C$ and $^{18}O/^{16}O$ ratios of modem land-snail shells from the southern great plains of North America. *Quaternary Research* **63**, 15-30.

Baldini, L.M., Walker, S.E., Railsback, L.B., Baldini, J.U.L., Crowe, D.E. (2007) Isotopic Ecology of the Modern Land Snail Cerion, San Salvador, Bahamas: Preliminary Advances toward Establishing a Low-Latitude Island Paleoenvironmental Proxy. *Palaios* **22**, 174-187.

Bao, R., Sheng, X., Teng, H.H., Ji, J. (2018) Reliability of shell carbon isotope composition of different land snail species as a climate proxy: A case study in the monsoon region of China. *Geochimica et Cosmochimica Acta* **228**, 42-61.

Bonadonna, F., Leone, G. (1995) Palaeoclimatological reconstruction using stable isotope data on continental molluscs from Valle di Castiglione, Roma, Italy. *Holocene* **5**, 461-469.

Bonifacie, M., Calmels, D., Eiler, J.M., Horita, J., Chaduteau, C., Vasconcelos, C., Agrinier, P., Katz, A., Passey, B.H., Ferry, J.M., Bourrand, J.-J. (2017) Calibration of the dolomite clumped isotope thermometer from 25 to 350 ^{o}C, and implications for a universal calibration for all (Ca, Mg, Fe) CO_3 carbonates. *Geochimica Et Cosmochimica Acta* **200**, 255-279.

Brand, W.A., Assonov, S.S., Coplen, T.B. (2010) Correction for the ^{17}O interference in $\delta(^{13}C)$ measurements when analyzing CO_2 with stable isotope mass spectrometry (IUPAC Technical Report). *Pure & Applied Chemistry* **82**, 1719-1733.

Cheng, H., Edwards, R.L., Sinha, A., Spötl, C., Yi, L., Chen, S., Kelly, M., Kathayat, G., Wang, X., Li, X. (2016) The Asian monsoon over the past 640,000 years and ice age terminations. *Nature* **534**, 640-646.

Colonese, A.C., Zanchetta, G., Fallick, A.E., Manganelli, G., Cascio, P.L., Hausmann,

N., Baneschi, I., Regattieri, E. (2014) Oxygen and carbon isotopic composition of modern terrestrial gastropod shells from Lipari Island, Aeolian Archipelago (Sicily). *Palaeogeography Palaeoclimatology Palaeoecology* **394**, 119-127.

Colonese, A.C., Zanchetta, G., Fallick, A.E., Manganelli, G., Sana, M., Alcalde, G., Nebot, J. (2013) Holocene snail shell isotopic record of millennial-scale hydrological conditions in western Mediterranean: Data from Bauma del Serrat del Pont (NE Iberian Peninsula). *Quaternary International* **303**, 43-53.

Colonese, A.C., Zanchetta, G., Fallick, A.E., Martini, F., Manganelli, G., Drysdale, R.N. (2010) Stable isotope composition of *Helix ligata* (Müller, 1774) from Late Pleistocene–Holocene archaeological record from Grotta della Serratura (Southern Italy): Palaeoclimatic implications. *Global & Planetary Change* **71**, 249-257.

Daeron, M., Blamart, D., Peral, M., Affek, H.P. (2016) Absolute isotopic abundance ratios and the accuracy of Δ_{47} measurements. *Chemical Geology* **442**, 83-96.

Dennis, K.J., Affek, H.P., Passey, B.H., Schrag, D.P., Eiler, J.M. (2011) Defining an absolute reference frame for 'clumped' isotope studies of CO_2. *Geochimica Et Cosmochimica Acta* **75**, 7117-7131.

Eagle, R.A., Risi, C., Mitchell, J.L., Eiler, J.M., Seibt, U., Neelin, J.D., Li, G., Tripati, A.K. (2013) High regional climate sensitivity over continental China constrained by glacial-recent changes in temperature and the hydrological cycle. *Proceedings of the National Academy of Sciences of the United States of America* **110**, 8813-8818.

Eide, M., Olsen, A., Ninnemann, U.S., Eldevik, T. (2017) A global estimate of the full oceanic ^{13}C Suess effect since the preindustrial. *Global Biogeochemical Cycles* 31, 492-514.

Eiler, J.M., Schauble, E. (2004) $^{18}O^{13}C^{16}O$ in Earth's atmosphere. *Geochimica Et Cosmochimica Acta* 68, 4767-4777.

Eiler, J.M. (2007) "Clumped-isotope" geochemistry - The study of naturally-occurring, multiply-substituted isotopologues. *Earth and Planetary Science Letters* **262**, 309-327.

Ghosh, P., Adkins, J., Affek, H., Balta, B., Guo, W.F., Schauble, E.A., Schrag, D., Eller, J.M. (2006) ^{13}C-^{18}O bonds in carbonate minerals: A new kind of paleothermometer. *Geochimica Et Cosmochimica Acta* **70**, 1439-1456.

Goodfriend, A.G., Hood, G.D. (1983) Carbon isotope analysis of land snail shells; implications for carbon sources and radiocarbon dating. *Radiocarbon* **25**, 810-830.

Goodfriend, A.G., Stipp, J.J. (1983) Limestone and the problem of radiocarbon dating of land-snail shell carbonate. *Geology* **11**, 575-577.

Goodfriend, G.A. (1992) The use of land snail shells in paleoenvironmental reconstruction. *Quaternary Science Reviews* **11**, 665-685.

Goodfriend, G.A., Ellis, G.L. (2000) Stable carbon isotope record of middle to late Holocene climate changes from land snail shells at Hinds Cave, Texas. *Quaternary International* **67**, 47-60.

Goodfriend, G.A., Ellis, G.L. (2002) Stable carbon and oxygen isotopic variations in

modern Rabdotus land snail shells in the southern Great Plains, USA, and their relation to environment. *Geochimica Et Cosmochimica Acta* **66**, 1987-2002.

Goodfriend, G.A., Magaritz, M. (1987) Carbon and oxygen isotope composition of shell carbonate of desert land snails. *Earth & Planetary Science Letters* **86**, 377-388.

Goodfriend, G.A., Magaritz, M., Gat, J.R. (1989) Stable isotope composition of land snail body water and its relation to environmental waters and shell carbonate. *Geochimica Et Cosmochimica Acta* **53**, 3215-3221.

Guo, Y., Deng, W., Wei, G., Lo, L., Wang, N. (2019) Clumped isotopic signatures in land-snail shells revisited: Possible palaeoenvironmental implications. *Chemical Geology* 519, 83-94.

Huang, L.P., Wu, N.Q., Gu, Z.Y., Chen, X.Y. (2012) Variability of snail growing season at the Chinese Loess Plateau during the last 75 ka. *Chinese Science Bulletin* **57**, 1036-1045.

Kehrwald, N.M., McCoy, W.D., Thibeault, J., Burns, S.J., Oches, E.A. (2010) Paleoclimatic implications of the spatial patterns of modern and LGM European land-snail shell $\delta^{18}O$. *Quaternary Research* **74**, 166-176.

Kelson, J.R., Huntington, K.W., Schauer, A.J., Saenger, C., Lechler, A.R. (2017) Toward a universal carbonate clumped isotope calibration: Diverse synthesis and preparatory methods suggest a single temperature relationship. *Geochimica Et Cosmochimica Acta* **197**, 104-131.

Kim, S.T., O'Neil, J.R., Hillaire-Marcel, C., Mucci, A. (2007) Oxygen isotope

fractionation between synthetic aragonite and water: Influence of temperature and Mg^{2+} concentration. *Geochimica Et Cosmochimica Acta* **71**, 4704-4715.

Kohn, M.J. (2010) Carbon isotope compositions of terrestrial C3 plants as indicators of (paleo)ecology and (paleo)climate. *Proc Natl Acad Sci U S A* **107**, 19691-19695.

Lécolle, P. (1985) The oxygen isotope composition of landsnail shells as a climatic indicator: Applications to hydrogeology and paleoclimatology. *Chemical Geology Isotope Geoscience* **58**, 157-181.

Liu, T.S., 1985. Loess and the Environment. China Ocean Press, Beijing, pp. 251.

Liu, W.G., Feng, X.H., Ning, Y.F., zhang, Q.L., Cao, Y.N., An, Z.S. (2005) $\delta^{13}C$ variation of C_3 and C_4 plants across an Asian monsoon rainfall gradient in arid northwestern China. *Global Change Biology* **11**, 1094-1100.

Liu, Z.X., Zhaoyan, G.U., Naiqin, W.U., Bing, X.U. (2007) Diet control on carbon isotopic composition of land snail shell carbonate. *Chinese Science Bulletin* **52**, 388-394.

Lu, Y.C., Wang, X.L., Wintle, A.G. (2007) A new OSL chronology for dust accumulation in the last 130,000 yr for the Chinese Loess Plateau. *Quaternary Research* 67, 152-160.

Metref, S., Rousseau, D.D., Bentaleb, I., Labonne, M., Vianey-Liaud, M. (2003) Study of the diet effect on $\delta^{13}C$ of shell carbonate of the land snail *Helix aspersa* in experimental conditions. *Earth & Planetary Science Letters* **211**, 381-393.

O'Leary, M.H. (1981) Carbon isotope fractionation in plants. Phytochemistry 20,

553-567.

Petersen, S.V., Defliese, W.F., Saenger, C., Daëron, M., Huntington, K.W., John, C.M., Kelson, J.R., Bernasconi, S.M., Colman, A.S., Kluge, T., Olack, G.A., Schauer, A.J., Bajnai, D., Bonifacie, M., Breitenbach, S.F.M., Fiebig, J., Fernandez, A.B., Henkes, G.A., Hodell, D., Katz, A., Kele, S., Lohmann, K.C., Passey, B.H., Peral, M.Y., Petrizzo, D.A., Rosenheim, B.E., Tripati, A., Venturelli, R., Young, E.D., Winkelstern, I.Z. (2019) Effects of Improved ^{17}O Correction on Interlaboratory Agreement in Clumped Isotope Calibrations, Estimates of Mineral-Specific Offsets, and Temperature Dependence of Acid Digestion Fractionation. *Geochemistry, Geophysics, Geosystems*. https://doi.org/10.1029/2018GC008127.

Pigati, J.S., Quade, J., Shahanan, T.M., Haynes, C.V. (2004) Radiocarbon dating of minute gastropods and new constraints on the timing of late Quaternary spring-discharge deposits in southern Arizona, USA. *Palaeogeography, Palaeoclimatology, Palaeoecology* **204**, 33-45.

Prendergast, A.L., Stevens, R.E., Barker, G., O'Connell, T.C. (2015) Oxygen isotope signatures from land snail (Helix melanostoma) shells and body fluid: Proxies for reconstructing Mediterranean and North African rainfall. *Chemical Geology* **409**, 87-98.

Prendergast, A.L., Stevens, R.E., Hill, E.A., Hunt, C., O'Connell, T.C., Barker, G.W. (2017) Carbon isotope signatures from land snail shells: Implications for palaeovegetation reconstruction in the eastern Mediterranean. *Quaternary International* **432**, 48-57.

Prendergast, A.L., Stevens, R.E., O'Connell, T.C., Hill, E.A., Hunt, C.O., Barker, G.W. (2016) A late Pleistocene *refugium* in Mediterranean North Africa? Palaeoenvironmental reconstruction from stable isotope analyses of land snail shells (Haua Fteah, Libya). *Quaternary Science Reviews* **139**, 94-109.

Quarta, G., Romaniello, L., Elia, M.D., Mastronuzzi, G., Calcagnile, L. (2007) Radiocarbon age anomalies in pre-and post-bomb land snails from the coastal Mediterranean basin. *Radiocarbon* **49**, 817-826.

Romanek, C.S., Grossman, E.L., Morse, J.W. (1992) Carbon isotopic fractionation in synthetic aragonite and calcite: Effects of temperature and precipitation rate. *Geochimica Et Cosmochimica Acta* **56**, 419-430.

Romaniello, L., Quarta, G., Mastronuzzi, G., D'Elia, M., Calcagnile, L. (2008) ^{14}C age anomalies in modern land snails shell carbonate from Southern Italy. *Quaternary Geochronology* **3**, 68-75.

Rousseau, D.D., Wu, N. (1997) A new molluscan record of the monsoon variability over the past 130 000 yr in the Luochuan loess sequence, China. *Geology* **25**, 275.

Rozanski, K., Araguás-Araguás, L., Gonfiantini, R. (1992) Relation between long-term trends of oxygen-18 isotope composition of precipitation and climate. *Science* **258**, 981-985.

Schauer, A.J., Kelson, J., Saenger, C., Huntington, K.W. (2016) Choice of ^{17}O correction affects clumped isotope (Δ_{47}) values of CO_2 measured with mass spectrometry. *Rapid Communications in Mass Spectrometry* **30**, 2607-2616.

Schmitt, J., Schneider, R., Elsig, J., Leuenberger, D., Lourantou, A., Chappellaz, J., Köhler, P., Joos, F., Stocker, T.F., Leuenberger, M., Fischer, H. (2012) Carbon isotope constraints on the deglacial CO_2 rise from ice cores. *Science* **336**, 711.

Stott, D.L. (2002) The influence of diet on the $\delta^{13}C$ of shell carbon in the pulmonate snail *Helix aspersa*. *Earth and Planetary Science Letters* **195**, 249-259.

Thompson, R., Cheny, S. (1996) Raising snails. National Agriculture Library Special reference briefs. NAL SRB 96-05.

Wang, G., Li, J., Liu, X., Li, X. (2013) Variations in carbon isotope ratios of plants across a temperature gradient along the 400mm isoline of mean annual precipitation in north China and their relevance to paleovegetation reconstruction. *Quaternary Science Reviews* **63**, 83-90.

Wang, X., Cui, L., Zhai, J., Ding, Z. (2016) Stable and clumped isotopes in shell carbonates of land snails *Cathaica sp* and *Bradybaena sp* in north China and implications for ecophysiological characteristics and paleoclimate studies. *Geochemistry Geophysics Geosystems* **17**, 219-231.

Wen, X.F., Wang, J.L., Hu, Z.M., Li, S.G., Yu, G.R. (2012) Dew water isotopic ratios and their relationships to ecosystem water pools and fluxes in a cropland and a grassland in China. *Oecologia* **168**, 549-561.

Wu, B. (2011) Terrestrial mollusk record from the Chinese Loess Plateau during the Middle Pleistocene Transition and its implications for paleoenvironmental evolution. Ph. D. Dissertation, in Chinese with English abstract, P. 1-96.

Wu, N., Li, F., Rousseau, D.D. (2018) Terrestrial mollusk records from Chinese loess

sequences and changes in the East Asian monsoonal environment. *Journal of Asian Earth Sciences* **155**, 35-48.

Wu, N.Q., Liu, T., Liu, X., Gu, Z. (2002) Mollusk record of millennial climate variability in the Loess Plateau during the Last Glacial Maximum. *Boreas* **31**, 20–27.

Xu, B., Gu, Z., Han, J., Hao, Q., Lu, Y., Wang, L., Wu, N., Pei, Y. (2011) Radiocarbon age anomalies of land snail shells in the Chinese Loess Plateau. *Quaternary Geochronology* **6**, 383-389.

Xu, W.H., Zhou, J.C., Zhang, E., Chen, Y.X., Yan, K.H., Wang, R.M. (2002) Effects of temperature and humidity on *Bradybeana similaris*. *Jiangsu Journal of Agriculture Science* **18**, 99-102.

Yanes, Y., Delgado, A., Castillo, C., Alonso, M.R., Ibáñez, M., Nuez, J.D.L., Kowalewski, M. (2008) Stable isotope ($\delta^{18}O$, $\delta^{13}C$, and δD) signatures of recent terrestrial communities from a low-latitude, oceanic setting: Endemic land snails, plants, rain, and carbonate sediments from the eastern Canary Islands. *Chemical Geology* **249**, 377-392.

Yanes, Y., Gómez-Puche, M., Esquembre-Bebia, M.A., Fernández-López-De-Pablo, J. (2013a) Younger Dryas – early Holocene transition in the south-eastern Iberian Peninsula: insights from land snail shell middens. *Journal of Quaternary Science* **28**, 777-788.

Yanes, Y., García-Alix, A., Asta, M.P., Ibáñez, M., Alonso, M.R., Delgado, A. (2013b) Late Pleistocene–Holocene environmental conditions in Lanzarote (Canary

Islands) inferred from calcitic and aragonitic land snail shells and bird bones. *Palaeogeography Palaeoclimatology Palaeoecology* **378**, 91-102.

Yanes, Y., Izeta, A.D., Cattáneo, R., Costa, T., Gordillo, S. (2014) Holocene (~4.5-1.7 cal. kyr BP) paleoenvironmental conditions in central Argentina inferred from entire-shell and intra-shell stable isotope composition of land snails. *Holocene* **24**, 1193-1205.

Yanes, Y., Nekola, J.C., Rech, J.A., Pigati, J.S. (2017) Oxygen stable isotopic disparities among sympatric small land snail species from northwest Minnesota, USA. *Palaeogeography Palaeoclimatology Palaeoecology*. 485, 715–722.

Yanes, Y., Romanek, C.S., Delgado, A., Brant, H.A., Noakes, J.E., Alonso, M.R., Ibáñez, M. (2009) Oxygen and carbon stable isotopes of modern land snail shells as environmental indicators from a low-latitude oceanic island. *Geochimica Et Cosmochimica Acta* **73**, 4077-4099.

Yanes, Y., Yapp, C.J., Ibáñez, M., Alonso, M.R., Delgado, A. (2011) Pleistocene–Holocene environmental change in the Canary Archipelago as inferred from stable isotope composition of land snail shells. *Quaternary Research (Orlando)* **75**, 658-669.

Yapp, C.J. (1979) Oxygen and Carbon Isotope Measurements of Land Snail Shell Carbonate. *Geochimica Et Cosmochimica Acta* **43**, 629-635.Zaarur, S., Olack, G., Affek, H.P. (2011) Paleo-environmental implication of clumped isotopes in land snail shells. *Geochimica Et Cosmochimica Acta* **75**, 6859-6869.

Zanchetta, G., Leone, G., Fallick, A.E., Bonadonna, F.P., Zanchetta, G., Leone, G.,

Fallick, A.E., Bonadonna, F.P. (2005) Oxygen isotope composition of living land snail shells: Data from Italy. *Palaeogeography Palaeoclimatology Palaeoecology* **223**, 20-33.

Zhai, J., Wang, X., Qin, B., Cui, L., Zhang, S., Ding, Z. (2019) Clumped isotopes in land snail shells over China: Towards establishing a biogenic carbonate paleothermometer. *Geochimica et Cosmochimica Acta* 257, 68-79.

Zhang, J., Quay, P.D., Wilbur, D.O. (1995) Carbon isotope fractionation during gas-water exchange and dissolution of CO_2. *Geochimica Et Cosmochimica Acta* **59**, 107-114.

Zhang, N., Lin, M., Snyder, G.T., Kakizaki, Y., Yamada, K., Yoshida, N., Matsumoto, R. (2019) Clumped isotope signatures of methane-derived authigenic carbonate presenting equilibrium values of their formation temperatures. *Earth and Planetary Science Letters* 512, 207-213.

Zhang, N., Yamada, K., Kano, A., Matsumoto, R., Yoshida, N. (2018) Equilibrated clumped isotope signatures of land-snail shells observed from laboratory culturing experiments and its environmental implications. *Chemical Geology* **488**, 189-199.

Zhang, N., Yamada, K., Suzuki, N., Yoshida, N. (2014) Factors controlling shell carbon isotopic composition of land snail *Acusta despecta sieboldiana* estimated from laboratory culturing experiment. *Biogeosciences* **11**, 5335-5348.

Zhang, N., Yamada, K., Yoshida, N. (2018) Food water contribution to the oxygen isotope composition of land snail body water and its environmental implication.

Geochemistry Geophysics Geosystems 19, 1800-1808.

Zhang, Z., Li, G., Hong, Y., An, Z. (2017) Microcodium in Chinese loess as a recorder for the oxygen isotopic composition of monsoonal rainwater. *Quaternary International* **464**, 364-369.

Zhou, W., Feng, X., Du, Y., Kong, X., Wu, Z. (2014) The last 130 ka precipitation reconstruction from Chinese loess ^{10}Be. *Journal of Geophysical Research Solid Earth* **119**, 191-197.

Table and Figures

Table 1. Compiled clumped and stable isotope compositions ($\delta^{13}C_{shell}$, $\delta^{18}O_{shell}$, Δ_{47} and $\delta^{18}O_{water}$) of modern and fossil snail shells from Luochuan and Weinan on the Chinese Loess Plateau. There is only 1 measurement for each sample. Δ_{47} values are reported in the absolute carbon dioxide equilibrated scale (CDES) defined by Dennis et al. (2011) without fractionation correction for acid digestion at 90 ℃. Δ_{47} values are calculated with the ^{17}O correction parameters from Brand et al. (2010). The Δ_{47}–T calibration line of Peterson et al. (2019) is used to convert $\Delta_{47CDES90}$ to temperature (T_{47}). The $\delta^{18}O_{water}$ from which the snail shells precipitated is calculated using the aragonite–water fractionation factor from Kim et al. (2007) in combination with the T_{47} and $\delta^{18}O_{shell}$ of this study. "±1 S.E." = one internal standard error of the mean. * indicates the data analyzed in 2017, and other data were measured in 2012 at Caltech. # the shell size data are from the Ph.D. dissertation of Wu (2011). The black bold numbers show the mean values.

Table 1. Compiled Clumped and stable isotope compositions of modern and fossil snail shells.

Location	Depth (cm)	Species	Shell size (mm) height*width[#]	$\delta^{13}C$ ‰(VPDB)	$\delta^{18}O$ ‰(VPDB)	$\delta^{18}O_{body\ water}$ (VSMOW, ‰)	Δ_{47} CDES90 ‰	±1 S.E.	T_{47} (ºC)
	240	*Pupilla aeoli*	*3.5*1.5*	-6.359	-6.140	-5.846	0.620	0.016	19
	240	*Vallonia tenera*	*1*2.3*	-6.689	-5.616	-6.581	0.639	0.018	13
	280	*Pupilla aeoli*	*3.5*1.5*	-6.531	-6.040	-5.732	0.620	0.021	19
	280	*Vallonia tenera*	*1*2.3*	-7.807	-7.794	-7.570	0.621	0.021	18
	320	*Metodontia huaiensis*	*7~9*8~10*	-6.618	-8.262	-8.498	0.628	0.016	16
	320	*Metodontia huaiensis*	*7~9*8~10*	-6.290	-8.071	-6.436	0.600	0.018	25
Weinan	*320*	*Cathaica pulveratrix*	*20*22*	-6.541	-7.366	-8.389	0.640	0.017	12
	440	*Cathaica pulveratrix*	*20*22*	-6.745	-2.805	-3.230	0.631	0.017	15
	480	*Cathaica pulveratrix*	*20*22*	-6.587	-1.511	-2.790	0.643	0.008	11
	800	*Cathaica pulveraticula*	*6*10*	-6.091	-10.871	-8.809	0.594	0.017	27
	800	*Cathaica pulveratrix*	*20*22*	-7.482	-4.048	-4.692	0.634	0.020	14
	960	*Cathaica pulveraticula*	*6*10*	-8.435	-9.450	-10.934	0.647	0.018	10
	960	*Cathaica pulveratrix*	*20*22*	-6.941	-2.237	-2.278	0.625	0.018	17
				-6.855	**-6.955**	**-6.291**	**0.626**	**0.017**	**17**
	280	*Cathaica pulveratrix*	*20*22*	-6.193	-6.468	-7.148	0.634	0.013	14
	280	*Metodontia yantaiensis*	*6*8*	-7.973	-1.791	-0.496	0.605	0.019	23
	420	*Metodontia huaiensis*	*7~9*8~10*	-7.330	-6.465	-5.722	0.613	0.015	21
Luochuan	420	*Metodontia yantaiensis*	*6*8*	-7.973	-13.074	-13.321	0.628	0.012	16
	610	*Metodontia huaiensis*	*7~9*8~10*	-7.433	-8.223	-7.126	0.608	0.022	23
	610	*Cathaica pulveratrix*	*20*22*	-7.461	-1.436	-2.407	0.639	0.024	13
	730	*Pupilla aeoli*	*3.5*1.5*	-7.480	-7.504	-7.243	0.620	0.011	18

	730	*Metodontia huaiensis*	*7~9*8~10*	-9.082	-7.982	-6.898	0.608	0.016	22
	730	*Vallonia tenera*	*1*2.3*	-7.912	-8.687	-8.464	0.621	0.017	18
	860	*Metodontia huaiensis*	*7~9*8~10*	-9.035	-6.360	-6.639	0.628	0.021	16
	860	*Cathaica pulveratrix*	*20*22*	-7.207	-5.340	-5.437	0.626	0.017	17
	860	*Metodontia yantaiensis*	*6*8*	-8.279	-3.796	-3.977	0.627	0.018	16
	870	*Pupilla aeoli*	*3.5*1.5*	-7.613	-6.430	-8.200	0.651	0.020	9
	870	*Metodontia huaiensis*	*7~9*8~10*	-8.590	-9.950	-10.174	0.628	0.014	16
	870	*Vallonia tenera*	*1*2.3*	-8.507	-8.698	-10.001	0.644	0.025	11
	870	*Metodontia yantaiensis*	*6*8*	-8.460	-8.703	-9.071	0.630	0.023	15
	870	*Metodontia yantaiensis*	*6*8*	-8.777	-2.596	-2.832	0.628	0.013	16
	880	*Metodontia huaiensis*	*7~9*8~10*	-8.581	-6.700	-7.710	0.639	0.015	12
	880	*Metodontia yantaiensis*	*6*8*	-7.001	-2.578	-3.995	0.646	0.017	11
	880	*Metodontia yantaiensis*	*6*8*	-8.312	-7.860	-8.469	0.633	0.016	14
	880	*Metodontia yantaiensis*	*6*8*	-8.103	-9.085	-10.637	0.648	0.022	10
	890	*Pupilla aeoli*	*3.5*1.5*	-7.723	-6.704	-7.795	0.641	0.017	12
	900	*Pupilla aeoli*	*3.5*1.5*	-7.287	-6.363	-6.958	0.633	0.013	14
	900	*Metodontia huaiensis*	*7~9*8~10*	-8.077	0.248	0.377	0.622	0.016	18
	900	*Metodontia huaiensis*	*7~9*8~10*	-7.800	-5.359	-5.101	0.621	0.014	18
	900	*Metodontia huaiensis*	*7~9*8~10*	-8.842	-5.646	-7.053	0.645	0.018	11
	900	*Vallonia tenera*	*1*2.3*	-8.017	-7.935	-9.175	0.643	0.015	11
	900	*Metodontia yantaiensis*	*6*8*	-8.759	-9.292	-10.364	0.640	0.013	12
	900	*Metodontia yantaiensis*	*6*8*	-8.337	-4.238	-2.252	0.595	0.012	27
	900	*Metodontia yantaiensis*	*6*8*	-7.500	-4.753	-5.217	0.631	0.020	15
				-7.988	**-6.326**	**-6.650**	**0.629**	**0.017**	**16**
Weinan	Modern	*Bradybaena sp.*	*14*16*	-9.422	-2.162	-0.575	0.601	0.018	25
	Modern	*Bradybaena sp.*	*14*16*	-9.694	-5.157	-2.964	0.592	0.009	28

	Modern	*Bradybaena sp.* *	*14*16*	-11.521	-0.918	-0.197	0.614	0.008	21
	Modern	*Bradybaena sp.* *	*14*16*	-11.565	-0.903	2.088	0.581	0.017	32
	Modern	*Bradybaena sp.* *	*14*16*	-10.428	-2.414	1.927	0.563	0.024	39
	Modern	*Bradybaena sp.* *	*14*16*	-11.000	-1.128	0.004	0.608	0.016	23
	Modern	*Cathaica pulveraticula* *	*6*10*	-9.938	-8.216	-6.374	0.597	0.014	26
	Modern	*Cathaica pulveraticula* *	*6*10*	-10.068	-0.517	1.549	0.594	0.022	27
				-10.455	**-2.677**	**-0.568**	**0.594**	**0.016**	**28**
	Modern	*Bradybaena sp.*	*14*16*	-9.940	-3.506	-1.101	0.589	0.023	29
	Modern	*Bradybaena sp.*	*14*16*	-8.447	-5.464	-4.815	0.615	0.018	20
	Modern	*Bradybaena sp.* *	*14*16*	-11.201	-1.309	0.787	0.594	0.013	27
	Modern	*Bradybaena sp.* *	*14*16*	-14.566	-8.177	-4.373	0.570	0.023	36
Luochuan	Modern	*Bradybaena sp.* *	*14*16*	-10.680	-2.522	-0.022	0.588	0.019	30
	Modern	*Cathaica pulveraticula**	*6*10*	-8.929	-1.247	0.442	0.600	0.012	25
	Modern	*Cathaica pulveraticula* *	*6*10*	-9.111	-3.515	-1.782	0.599	0.019	26
	Modern	*Cathaica pulveraticula* *	*6*10*	-8.188	-9.444	-6.737	0.585	0.017	31
				-10.133	**-4.398**	**-2.200**	**0.592**	**0.018**	**28**

* indicates the shells analyzed in 2017 and others are measured in 2012

[#] the shell size data are from the Ph.D. dissertation of Wu (2011)

Figure 1. Map showing the sampling locations at Weinan and Luochuan (red filled circles).

Figure 2. Comparison of T_{47} in modern snail shells from Weinan (blue filled circles for *Bradybaena sp.* and blue crosses for *Cathaica pulveraticula*) and Luochuan (yellow filled circles for *Bradybaena sp.* and yellow crosses for *Cathaica pulveraticula*) with monthly average temperatures (filled black circles, monitored using HOBO Pro v2 loggers at Luochuan in 2016) and precipitation (gray bars, data from http://data.cma.cn/). The gray bar shows the measurement error for a single analysis. The dashed gray lines with triangles above and below the black line show the maximum and minimum temperatures, respectively. The left and right y-axes show the temperature and precipitation, respectively. The horizontal gray dashed line shows the mean T_{47} of all modern snails (28 ℃).

Figure 3. Comparison of magnetic susceptibility (MS) versus depth at the Weinan (red, top) and Luochuan (green, bottom) sections. The vertical gray dashed lines show the approximate boundary between marine isotope stages (MIS) based on previous dating studies (Lu et al., 2007), and lithology is shown in the top bar. The dashed lines with pink and purple filled circles show the mean T_{47} of at least two measurements of fossil snails from the Weinan and Luochuan sections, respectively. They show similar variations and suggest an increase of ~4 ℃ in T_{47} between MIS 4 and MIS 3, although the amplitude is on the same order of magnitude as the analytical precision. The

horizontal gray dashed lines denote the mean T_{47} of all modern snails (28 ℃).

Figure 4. Histograms of Δ_{47} temperature for fossil (top, blue) and modern (bottom, red) snail shells. The modern snail shell Δ_{47} temperature is ~10 ℃ higher than that of fossil snails.

Figure 5. Histograms of $\delta^{13}C$ for fossil (top, blue) and modern (bottom, red) snail shells.

Figure 6. Histograms of $\delta^{18}O$ for fossil (top, blue) and modern (bottom, red) snail shells.

Figure 7. Histograms of $\delta^{18}O$ of body water for the fossil (top, blue) and modern (bottom, red) snails. The water $\delta^{18}O$ is more positive for modern snail shells than for fossil shells.

Figure 8. The monthly mean precipitation (left, data from http://data.cma.cn/) and precipitation isotopes (right, data from http://isohis.iaea.org) at sites on/around the CLP. Precipitation is mainly concentrated from April to October, and the corresponding precipitation $\delta^{18}O$ mainly varies between -4‰ and -9‰.

Figure 9. Correlation between $\delta^{13}C$ and T_{47} for fossil and modern snail shells.

Different species are shown by different symbols, and modern snails are shown by red filled symbols.

Declaration of interests

☒ The authors declare that they have no known competing financial interests or personal relationships that could have appeared to influence the work reported in this paper.

☐The authors declare the following financial interests/personal relationships which may be considered as potential competing interests:

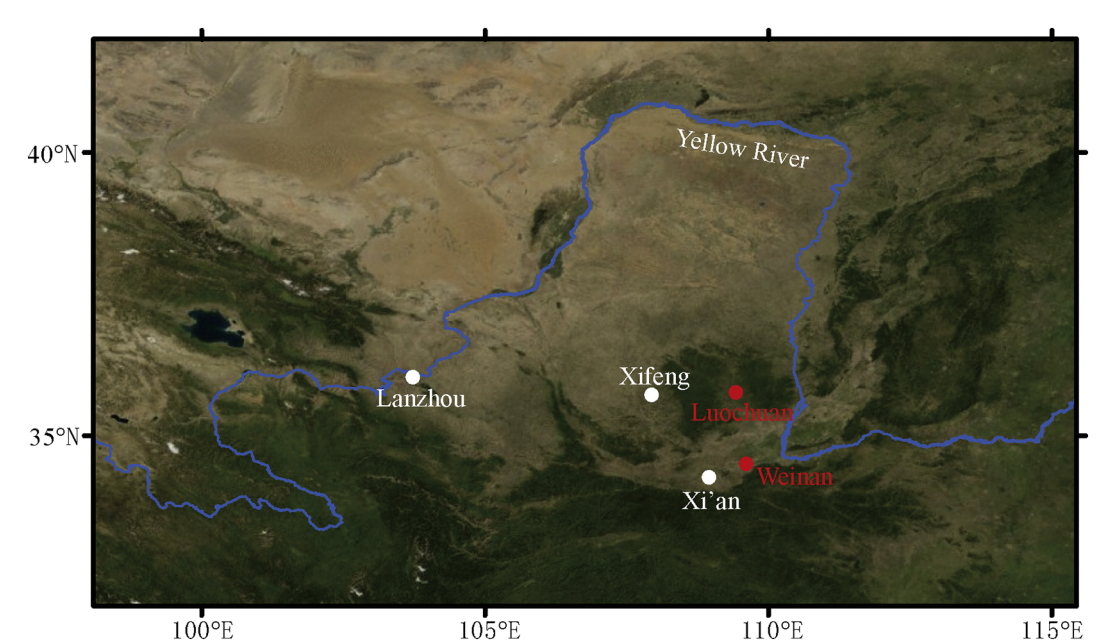
40°N
35°N
100°E
105°E
110°E
115°E
Yellow River
Lanzhou
Xifeng
Luochuan
Weinan
Xi'an

Figure 1

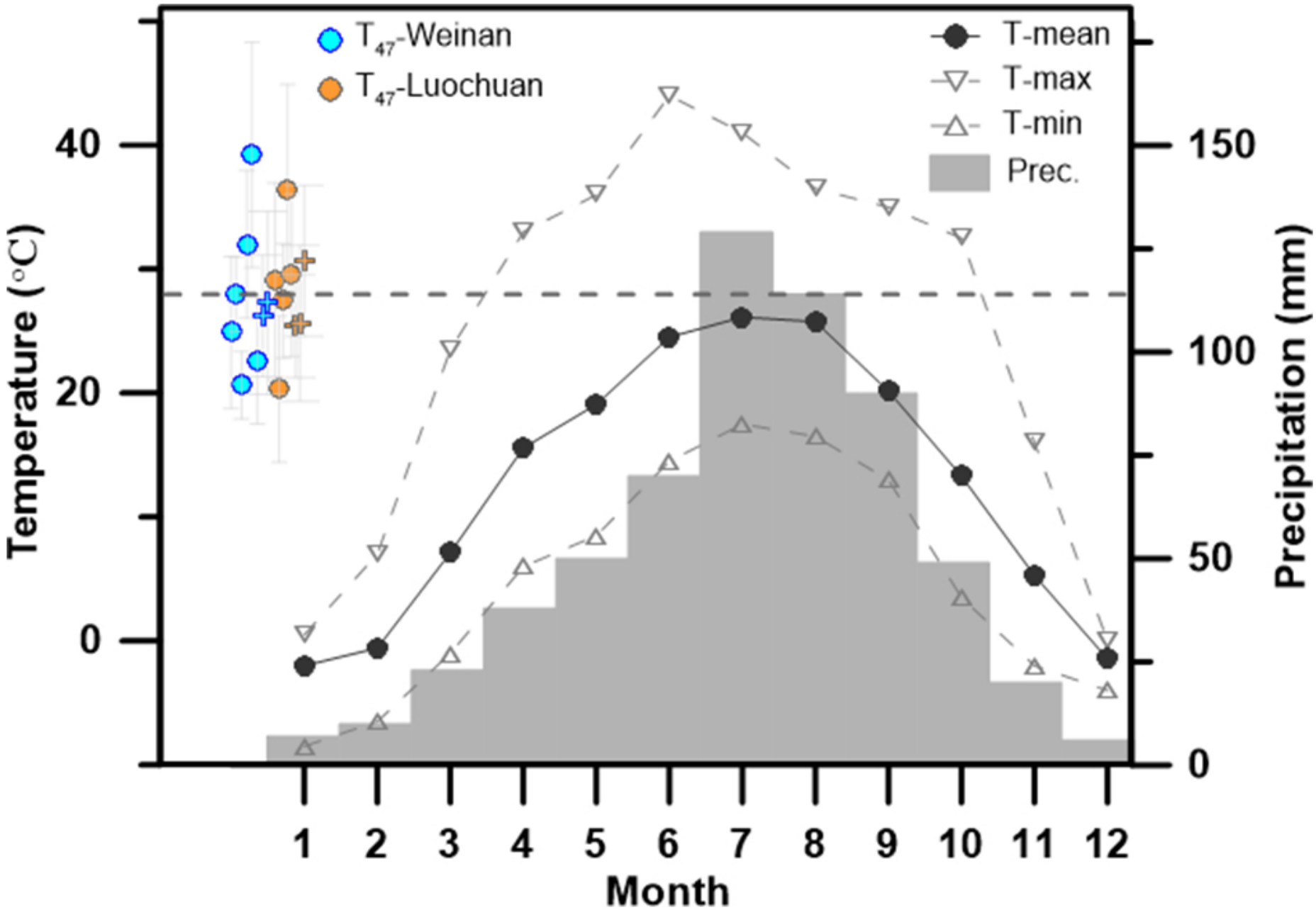
T47-Weinan
T47-Luochuan
T-mean
T-max
T-min
Prec.
Temperature (°C)
Precipitation (mm)
40
20
0
150
100
50
0
1
2
3
4
5
6
7
8
9
10
11
12
Month

Figure 2

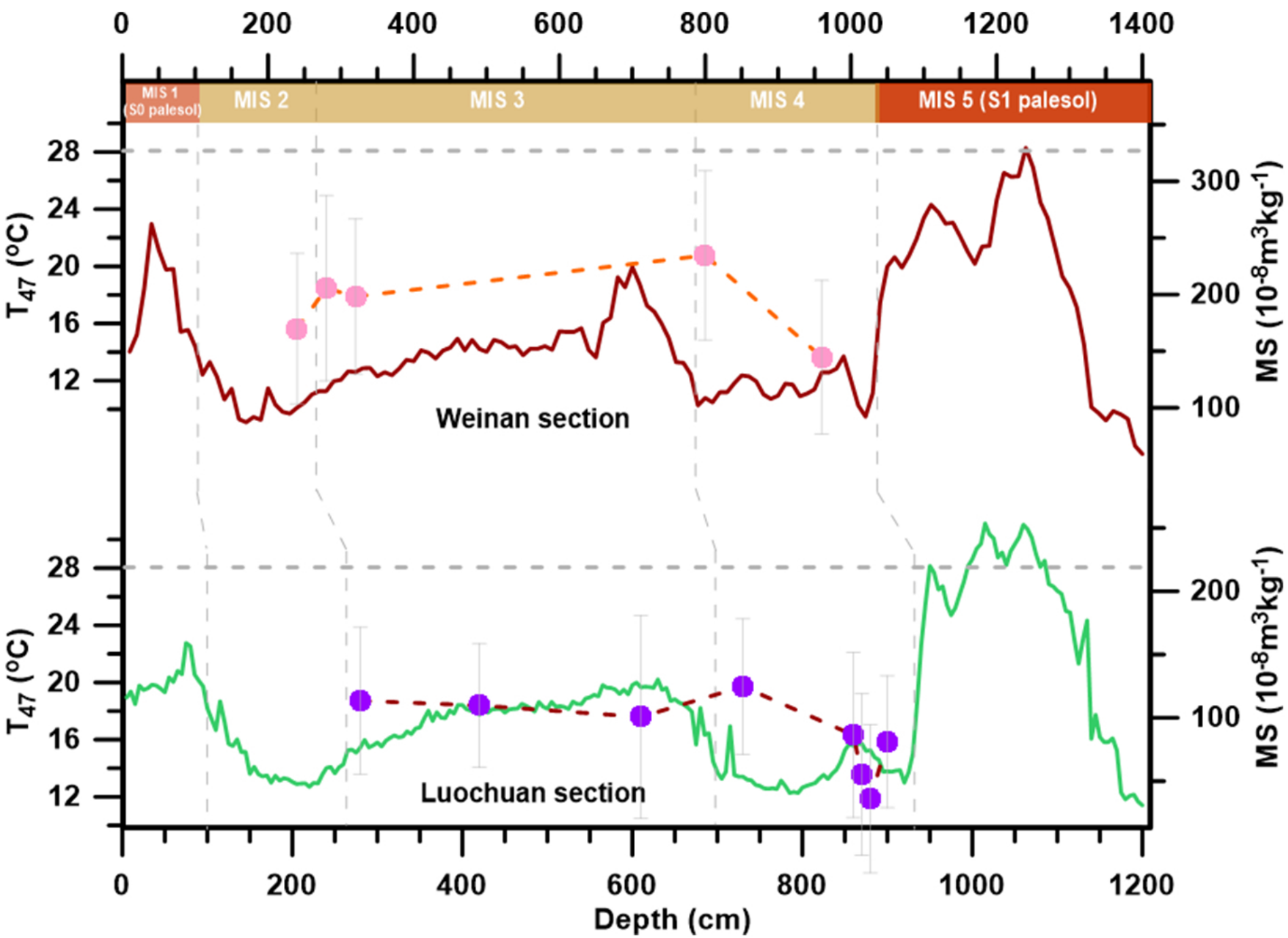
0
200
400
600
800
1000
1200
1400
MIS 1 (S0 palesol)
MIS 2
MIS 3
MIS 4
MIS 5 (S1 palesol)
28
24
20
16
12
T_{47} (°C)
300
200
100
MS ($10^{-8}m^3kg^{-1}$)
Weinan section
Luochuan section
Depth (cm)

Figure 3

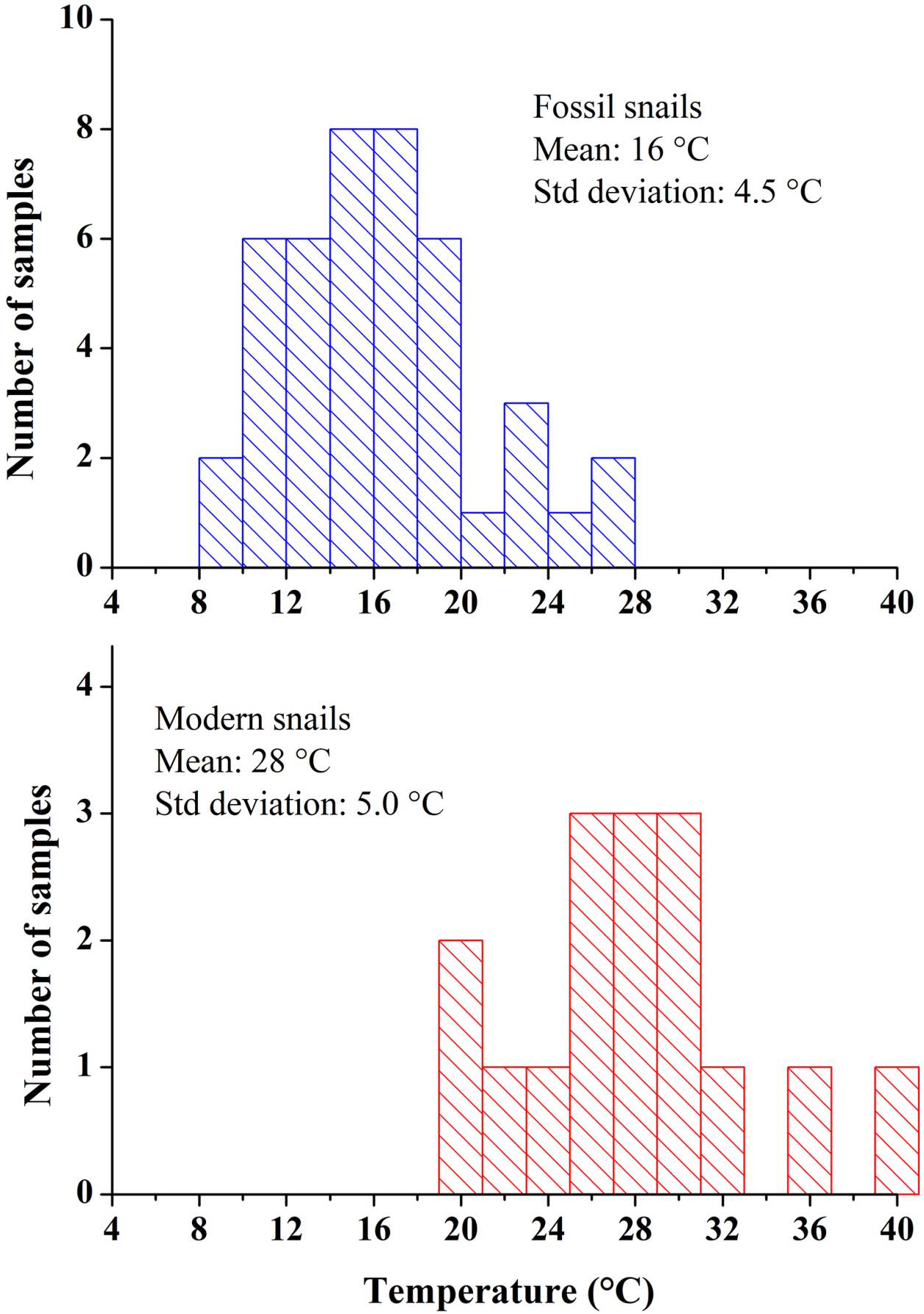
Fossil snails
Mean: 16 °C
Std deviation: 4.5 °C
Number of samples
Modern snails
Mean: 28 °C
Std deviation: 5.0 °C
Number of samples
Temperature (°C)

Figure 4

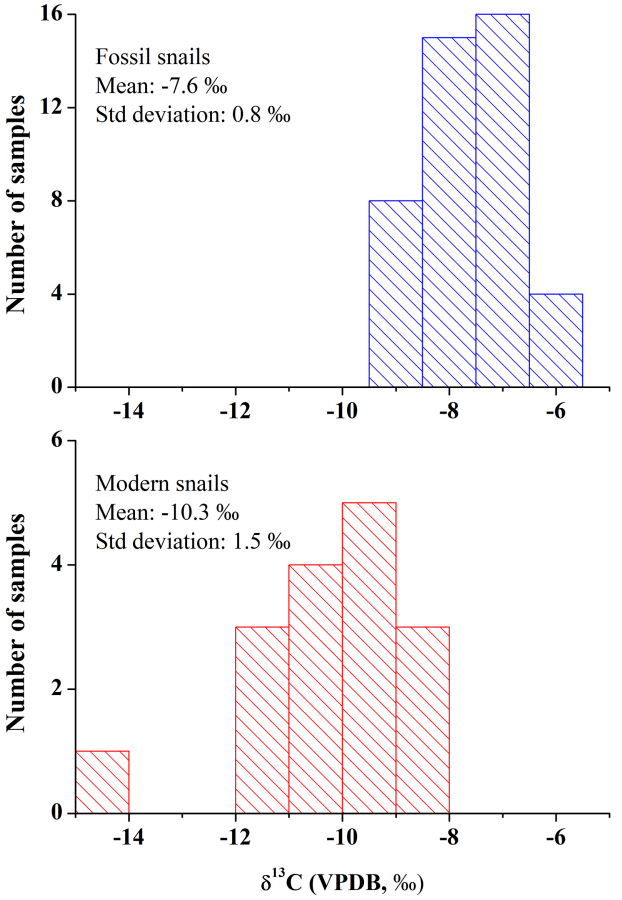
Fossil snails
Mean: -7.6 ‰
Std deviation: 0.8 ‰
Number of samples
16
12
8
4
0
-14
-12
-10
-8
-6
Modern snails
Mean: -10.3 ‰
Std deviation: 1.5 ‰
Number of samples
6
4
2
0
-14
-12
-10
-8
-6
δ13C (VPDB, ‰)

Figure 5

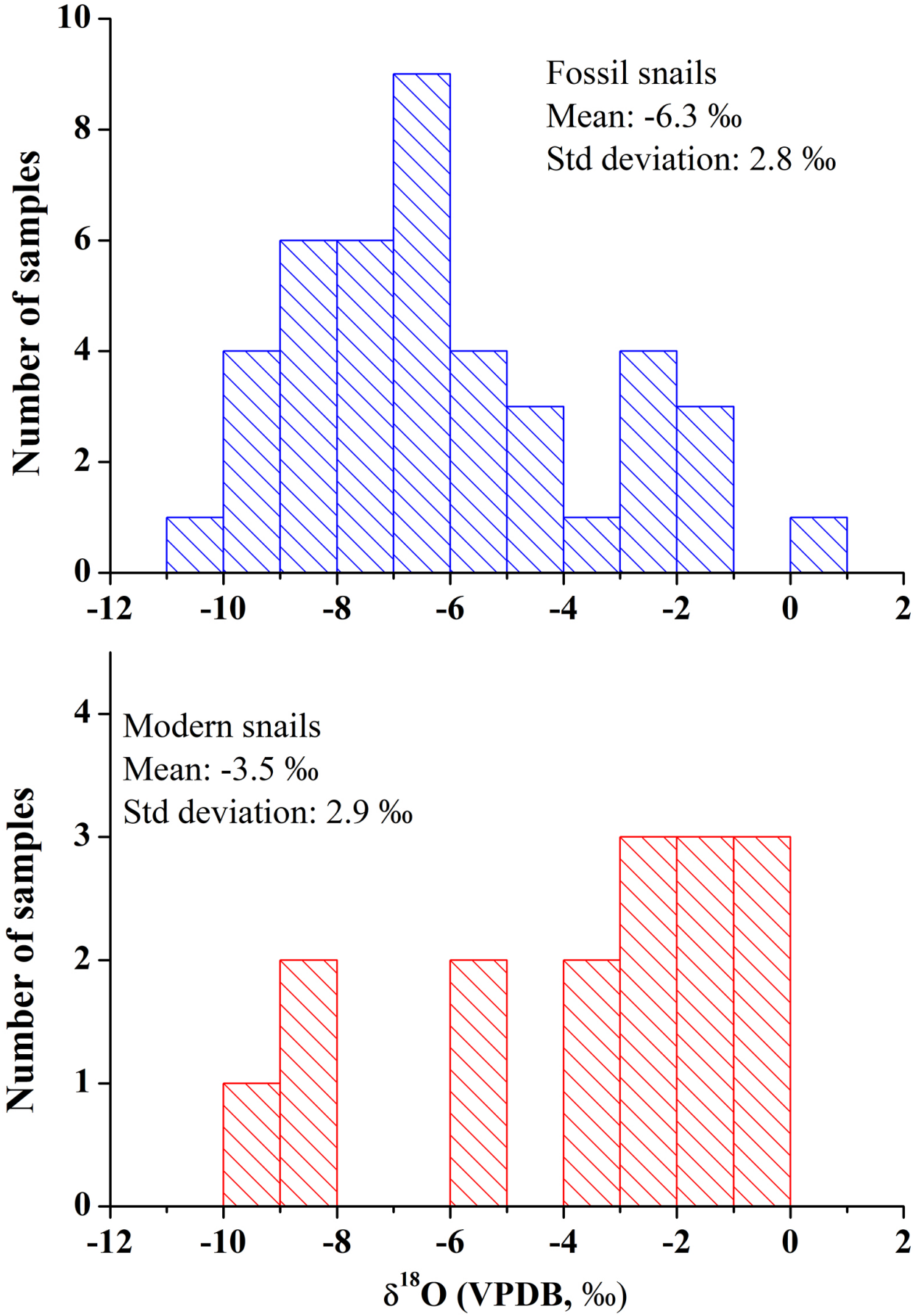
Fossil snails
Mean: -6.3 ‰
Std deviation: 2.8 ‰
Number of samples
Modern snails
Mean: -3.5 ‰
Std deviation: 2.9 ‰
Number of samples
δ18O (VPDB, ‰)

Figure 6

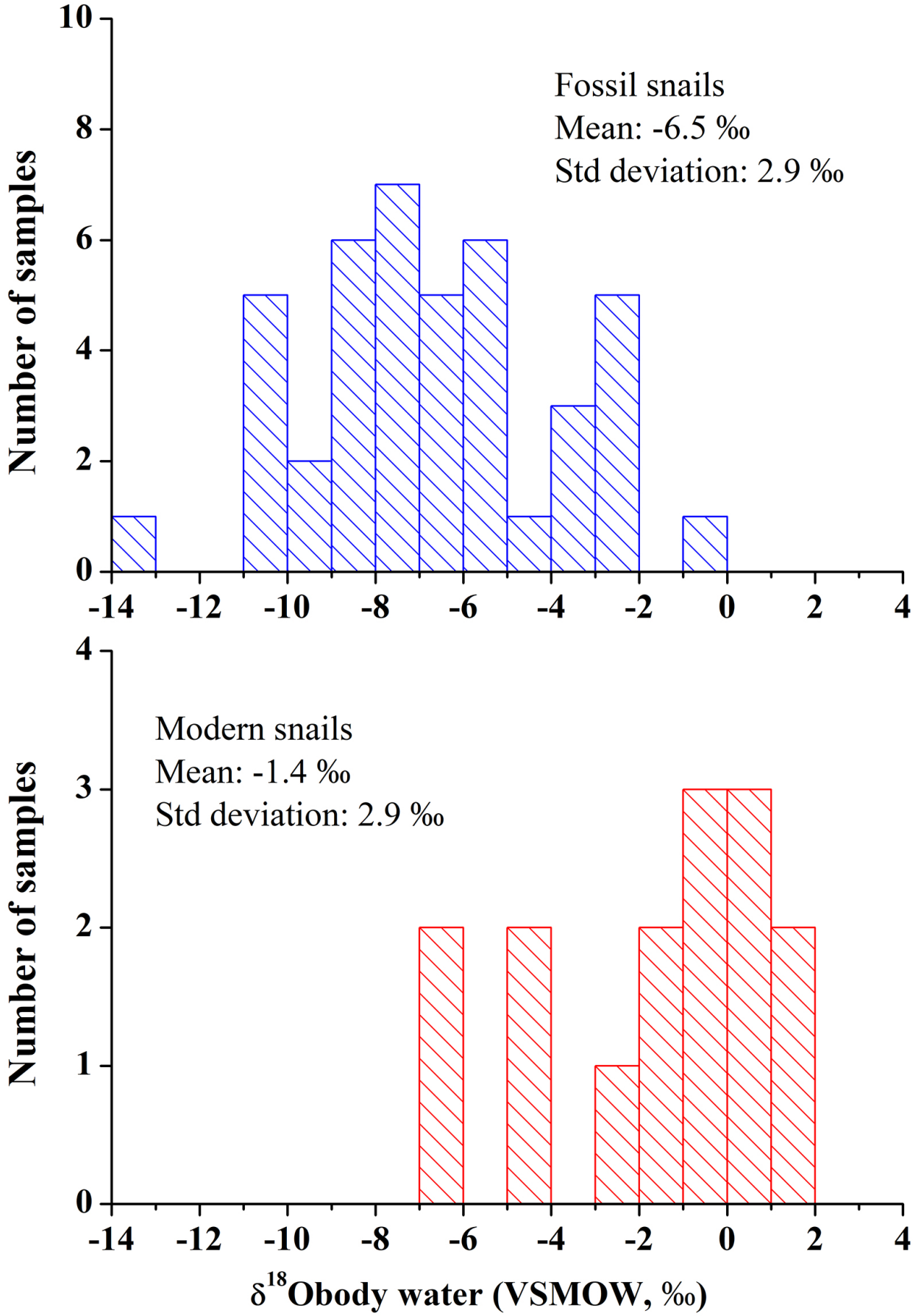
Fossil snails
Mean: -6.5 ‰
Std deviation: 2.9 ‰
Number of samples
Modern snails
Mean: -1.4 ‰
Std deviation: 2.9 ‰
Number of samples
δ18Obody water (VSMOW, ‰)

Figure 7

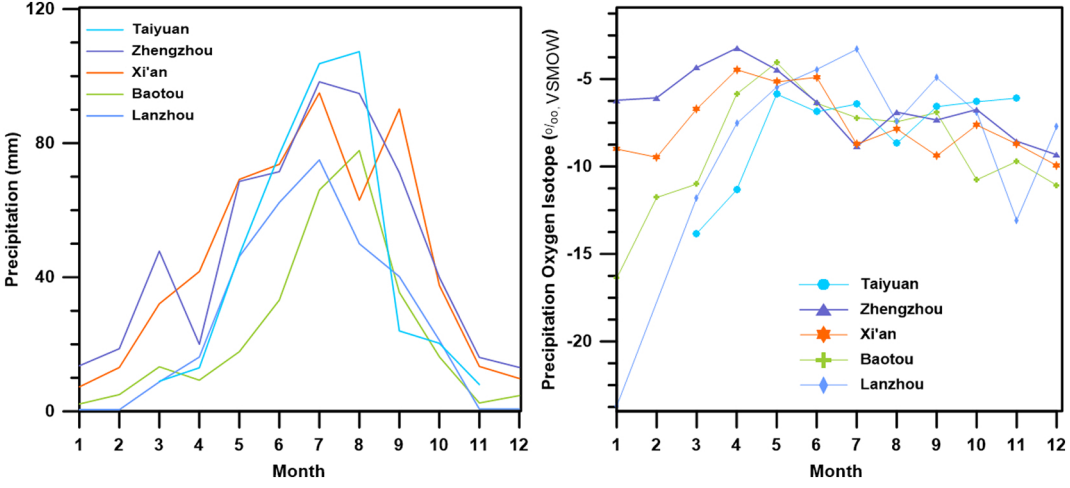
Taiyuan
Zhengzhou
Xi'an
Baotou
Lanzhou
Precipitation (mm)
120
80
40
0
1
2
3
4
5
6
7
8
9
10
11
12
Month
Precipitation Oxygen Isotope (‰, VSMOW)
-5
-10
-15
-20
Taiyuan
Zhengzhou
Xi'an
Baotou
Lanzhou
Month

Figure 8

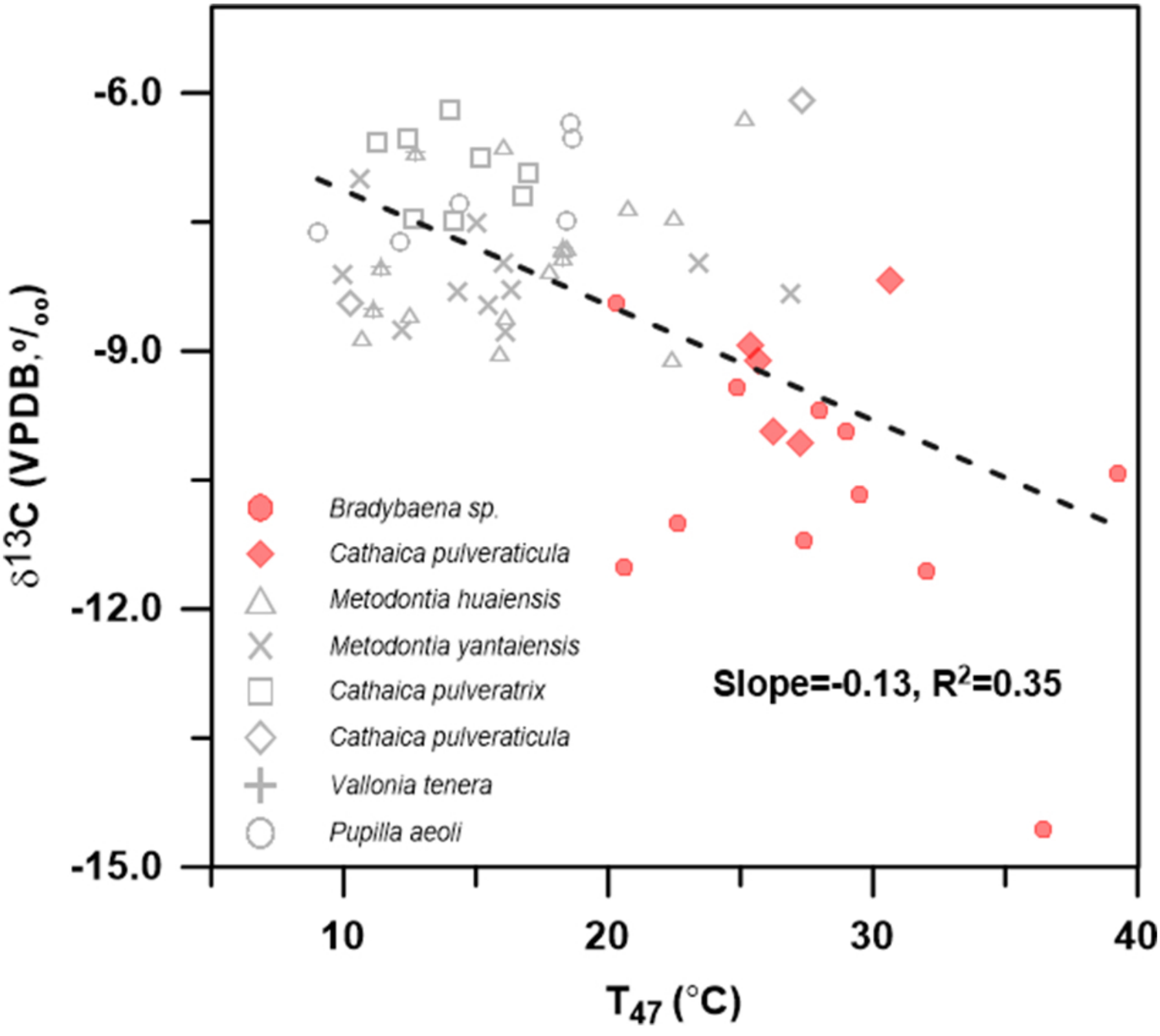
-6.0
-9.0
-12.0
-15.0
δ13C (VPDB,‰)
10
20
30
40
T47 (°C)
Bradybaena sp.
Cathaica pulveraticula
Metodontia huaiensis
Metodontia yantaiensis
Cathaica pulveratrix
Cathaica pulveraticula
Vallonia tenera
Pupilla aeoli
Slope=-0.13, R2=0.35

Figure 9

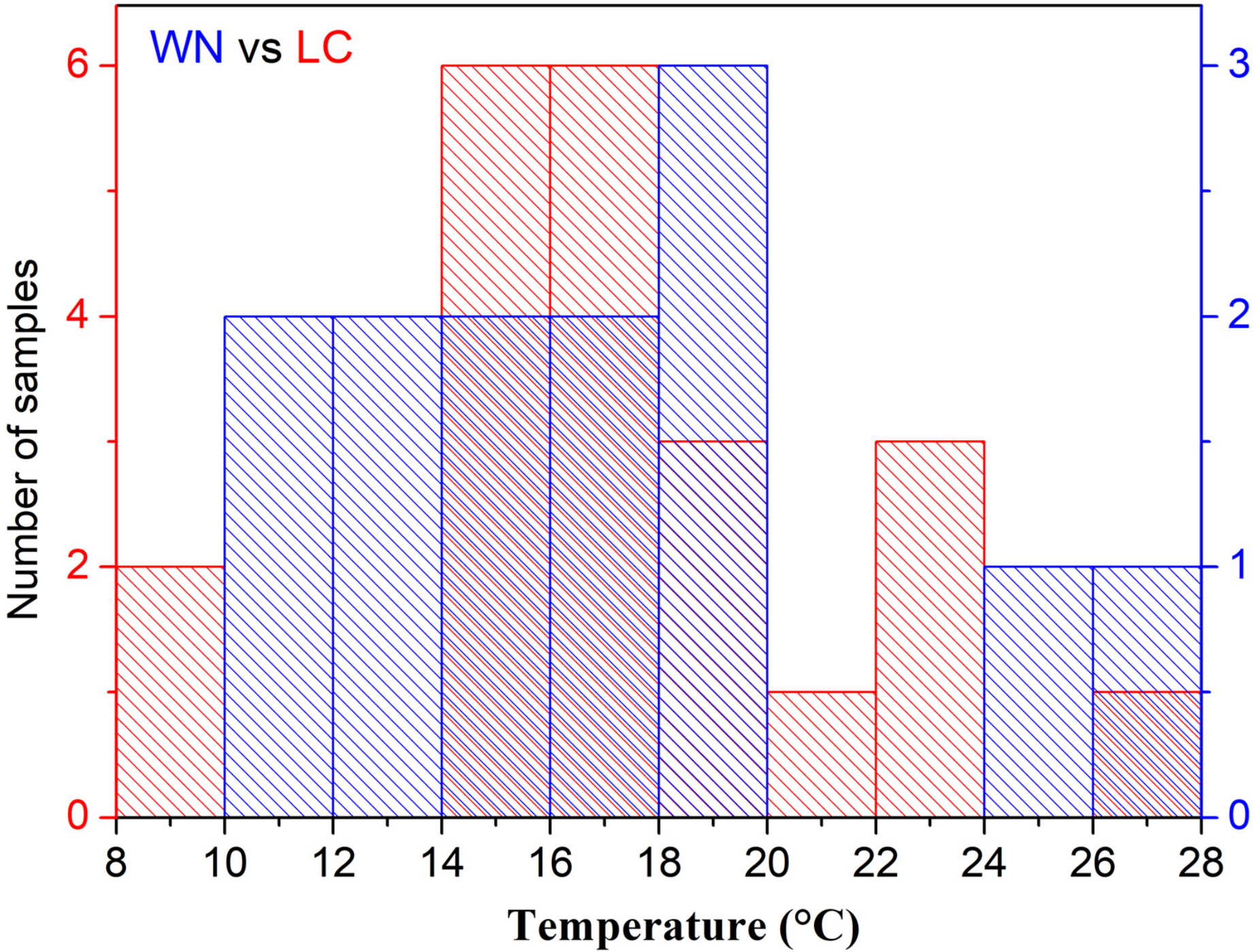
WN vs LC
Number of samples
Temperature (°C)
0
2
4
6
0
1
2
3
8
10
12
14
16
18
20
22
24
26
28

Figure 10

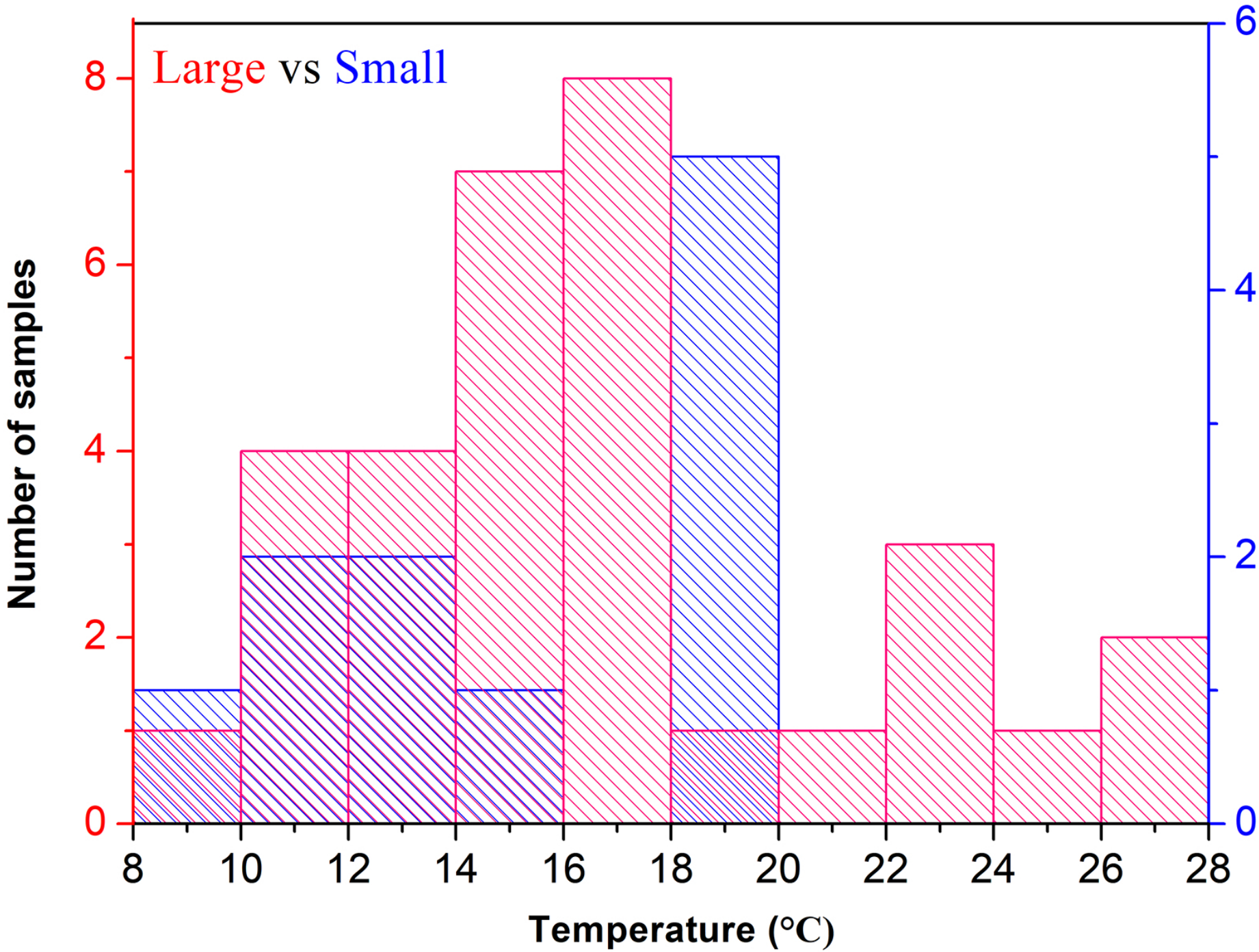
Large vs Small
Number of samples
Temperature (°C)
0
2
4
6
8
0
2
4
6
8
10
12
14
16
18
20
22
24
26
28

Figure 11